Optimal Control of Supersonic Inlet/Engine Combination

Jiahn-Bo Yarng* and Yan-Shen Guan†
Northwestern Polytechnical University, Xi'an, China

This paper applies the techniques of modern optimal control theory to the design of a contol system for a two-input, two-output inlet/engine combination. The mathematical model of the integrated combination is formulated using an idea of flow matching of the inlet and the engine. The control problem is approached as a stochastic linear quadratic regulator problem. The state estimator is designed by a recursive eigenvalue-eigenvector method for a linear time-invariant state equation. The results of a digital simulation for a NASA 48 cm inlet/J85 engine combination show that this design method is satisfactory.

Introduction

THE integrated two-variable control of a supersonic inlet/engine combination is one of the important problems in the development of high-performance supersonic propulsion systems. Cole et al.,[1] Paulovich et al.,[2] and Baumbick et al.[3] have studied this problem by analog simulation with stiff differential equations composed of a first-order lag element for the medium-frequency inlet shock dynamics and a first-order lag element of low-frequency engine dynamics. Actually, the medium-frequency transient behavior of the inlet shock dynamics has been greatly simplified and the transient behavior of many other important parameters (such as engine turbine inlet temperature, compressor outlet pressure, etc.) ignored. Lehtinen et al.,[4] Zeller et al.,[5] and Seidel et al.[6] have studied the linear stochastic optimal control of a supersonic inlet with a single input and a single output, both analytically and experimentally. Zeller[7] has given a comprehensive survey on the application of modern control theory to engine control. DeHoff and Hall[8] and Skira et al.[9] have presented their valuable works on the application of optimal control to the acceleration of aircraft turbine engines. Lee and Guan[10] have presented a paper on the optimal control of the change of state in an aircraft turbine engine. But the optimal control problem for a two-variable system has not yet been solved.

This paper is devoted to presenting an analytical design method for such an optimal control problem (see Fig. 1). The two-variable control consists of a constant shock position X_s control, and a constant engine speed N control. The weighted summation of variances in increments of the controlled variables (X_s and N) and of the control variables (inlet bypass door control U_{BP} and fuel flow rate W_F) is selected as the performance index.

Formulation of the Integrated Control Object

Figure 2 is a block diagram of this system. The integrated control system consists of two main components (inlet and engine) and three accessories (bypass door, actuator, and main fuel pump). Downstream stochastic airflow disturbance ΔW_w, shock position and rotor speed measurement stochastic disturbances ΔV_{XS} and ΔV_N, are taken into consideration.

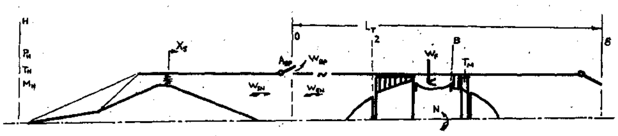

Fig. 1 Schematic diagram of the inlet/engine combination.

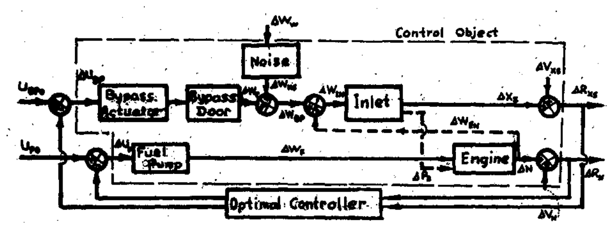

Fig. 2. Block diagram of the optimal control system of the inlet/engine combination.

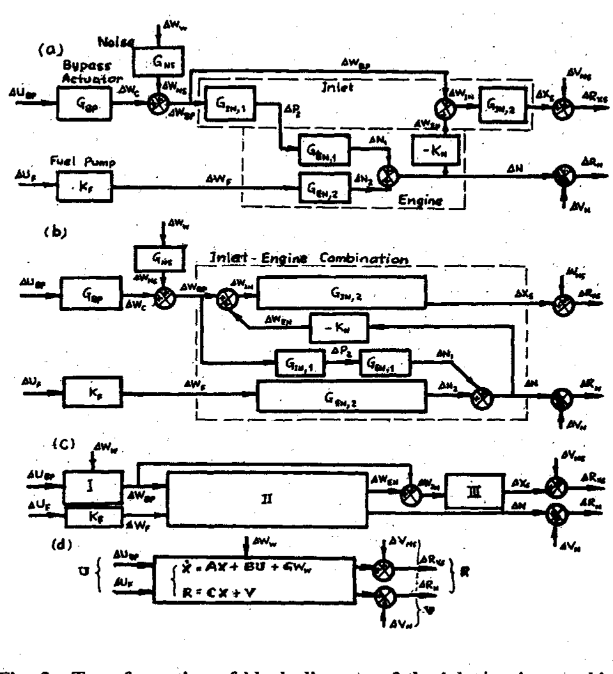

Fig. 3 Transformation of block diagram of the inlet/engine combination.

Received April 11, 1986; revision received April 21, 1987.

*Research Assistant, Department of Aero-Engine Engineering.
†Professor, Department of Aero-Engine Engineering.

Two-Variable State Space Model of the Combination

Applying the author's idea of Ref. 11, following the block diagrams of Figs. 2 and 3a, results in a mathematical model of each block, which can then be combined and transferred into one integrated block as shown in Fig. 3d.

Inlet Frequency Domain Model

Applying the method of Ref. 11, the transfer function of the inlet exit total pressure increment ΔP_2 from the bypass airflow increment ΔW_{BP} is

$$G_{IN,1} = \frac{\Delta P_2}{\Delta W_{BP}} = \frac{b_{61}S^5 + b_{51}S^4 + b_{41}S^3 + b_{31}S^2 + b_{21}S + b_{11}}{S^6 + a_{61}S^5 + a_{51}S^4 + a_{41}S^3 + a_{31}S^2 + a_{21}S + a_{11}} \quad (1)$$

and the transfer function of inlet shock position increment ΔX_s from inlet exit airflow rate increment ΔW_{IN} is

$$G_{IN,2} = \frac{\Delta X_S}{\Delta W_{IN}} = \frac{b_{12}}{S^6 + a_{62}S^5 + a_{52}S^4 + a_{42}S^3 + a_{32}S^2 + a_{22}S + a_{12}} \quad (2)$$

Equations (1) and (2) represent the dynamic responses of the downward and upward wave propagation of the flow disturbance, respectively. Because the denominators of the two inlet transfer functions $G_{IN,1}$ and $G_{IN,2}$ are different for the cross-sectional areas of the upward convergent portion X_S-A_{BP} and the downward extension duct portions 0-2 (see Fig. 1) are different, their volume dynamics are different. Each of them is a sixth-order model of part of the inlet. Their logarithmic amplitude vs frequency and phase vs frequency characteristics are different, as shown in Fig. 4. The whole inlet is of twelfth order and is a medium frequency (e.g., volume dynamics) model with a time constant of 0.01–0.05 s. The resultant upward and downward wave propagation effects have been included in a single sixth-order characteristic equation[5,12] for studying the inlet dynamics and its control only. Surely, the sixth-order transfer function $G_{IN,1}$ or $G_{IN,2}$ can be reduced to, say, third order by further approximation. But the accuracy will be greatly decreased.

Engine State Equation and Frequency Domain Model

A real engine covers a wide range of frequencies.[13] The rotor inertia and thermal lag of turbine blades represent low-frequency dynamics of the engine with a time constant of 0.1–1 s. The gas compressibilities of the compressor and turbine cascade volumes represent high-frequency dynamics of the engine with a time constant of 0.00001–0.001 s. Therefore, for simplicity, the high-frequency volume dynamics of the engine are ignored. The gas compressibilities of the combustion chamber and exhaust nozzle volumes and combustion delay also represent medium-frequency dynamics of the engine with a time constant of 0.01–0.03 s, but they are to be considered as a portion of the extension duct (L_T in Fig. 1) of the inlet for simplicity. Otherwise, the engine model will be very complex.

Under such assumptions, the engine state equation (with a control variable W_F and an intake condition P_2) can be deduced from the nonlinear dynamic model developed by using Seldner's generalized simulation techniques,[14]

$$\begin{bmatrix} \Delta\dot{N} \\ \Delta\dot{T}_M \end{bmatrix} = \begin{bmatrix} a'_{11} & a'_{12} \\ a'_{21} & a'_{22} \end{bmatrix} \begin{bmatrix} \Delta N \\ \Delta T_M \end{bmatrix} + \begin{bmatrix} b'_{11} \\ b'_{21} \end{bmatrix} \Delta W_F + \begin{bmatrix} b'_{12} \\ b'_{22} \end{bmatrix} \Delta P_2 \quad (3)$$

Eliminating terms $\dot{T}_M$ and T_M from Eq. (3) and then transforming them into transfer functions by Laplace transformation, we get

$$G_{EN,1} = \frac{\Delta N_1}{\Delta P_2} = \frac{d_{23}S + d_{13}}{S^2 + a_{24}S + a_{14}}$$
$$G_{EN,2} = \frac{\Delta N_2}{\Delta W_F} = \frac{b_{24}S + b_{14}}{S^2 + a_{24}S + a_{14}} \quad (4)$$

where

$$a_{14} = a'_{11}a'_{22} - a'_{12}a'_{21}, \qquad b_{24} = b'_{11}$$
$$a_{24} = -a'_{11} - a'_{22}, \qquad d_{13} = a'_{12}b'_{22} - a'_{22}b'_{21}$$
$$b_{14} = a'_{12}b'_{12} - a'_{22}b'_{11}, \qquad d_{23} = b'_{21}$$

and ΔN_1 and ΔN_2 are deviations in the engine speed due to the change of inlet exit pressure P_2 and fuel flow rate W_F.

Noise Model

The transfer function of the disturbance noise[5] is

$$G_{NS} = \frac{\Delta W_{NS}}{\Delta W_w} = \frac{d_{22}S + d_{12}}{S^2 + C_{22}S + C_{12}} \quad (5)$$

where $C_{12} = \alpha_1\alpha_3$, $C_{22} = \alpha_1 + \alpha_3$, $d_{12} = \alpha_1\alpha_3$, and $d_{22} = \alpha_1\alpha_3/\alpha_2$, in which α_1, α_2, and α_3 are noise coefficients.

Frequency Domain Model of Bypass Door and Actuator

From Ref. 5 the transfer function of the bypass airflow increment ΔW_c from the control increment ΔU_{BP} of the actuator is

$$G_{BP} = \frac{\Delta W_c}{\Delta U_{BP}} = \frac{d_{11}}{S^2 + C_{21}S + C_{11}} \quad (6)$$

Fuel Pump

The transfer function of the fuel pump is

$$\Delta W_F = K_F \Delta U_F \quad (7)$$

where K_F is the pump gain.

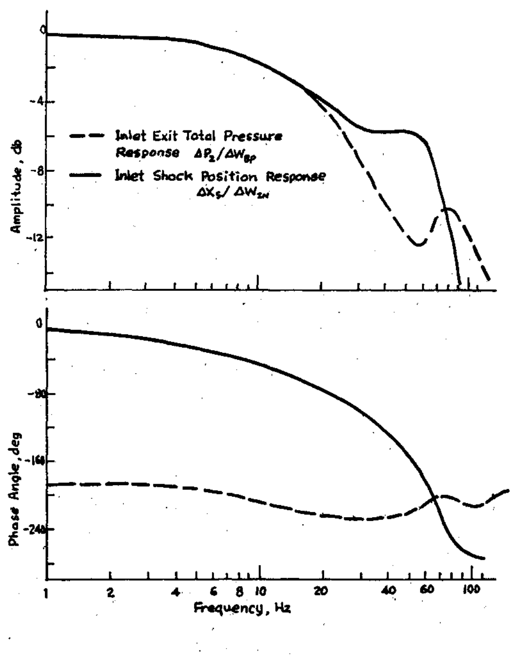

Fig. 4 Inlet frequency responses.

Formulation of Model of the Inlet/Engine Combination

By the law of continuity, the inlet airflow must be equal to the sum of the bypass airflow plus the engine airflow at bypass section 0 of Fig. 1 at any time, or

$$W_{IN} = W_{BP} + W_{EN} \tag{8}$$

During transient periods,

$$\Delta W_{IN} = \Delta W_{BP} + \Delta W_{EN} \tag{9}$$

This equation is the basis of flow matching between the inlet and the engine. As the bypass doors are opening, a signal of inlet exit (or engine intake) pressure increment ΔP_2 is transmitted to the engine as shown in Fig. 3. This signal induces a change of the engine speed ΔN. This is a forward-interacting signal of the inlet to the engine.

Similarily, as the engine speed changes, a signal of engine flow increment ΔW_{EN} is fed back to the inlet directly. This is a backward-interacting signal of the engine to the inlet as shown in Fig. 3.

Now, the block diagram of the inlet/engine combination as a control object (the block bounded by dotted lines in Fig. 2) can be transformed into Fig. 3a by substituting the transfer functions of Eqs. (1–6) into each corresponding block.

For small disturbance, the engine flow is proportional to the engine speed, or

$$\Delta W_{EN} = -K_N \Delta N \tag{10}$$

where K_N is the gain of the engine flow to the engine speed.

Then, the block diagram of Fig. 3a can be rearranged as Fig. 3b. However, the interacting transfer function $G_{IN,1}$ $G_{EN,1}$, and K_N of the two-input, and two-output inlet/engine combination are shown clearly.

The block diagram of Fig. 3 can be further simplified and transformed into Fig. 3c as shown. Block I is composed of the noise G_{NS} and the actuator G_{BP}, block II of the portion $G_{IN,1}$ of the inlet and the engine, and block III of the other portion $G_{IN,2}$ of the inlet. The state space model of the integrated combination is formulated by superposition of blocks I, II, and III as shown in Fig. 3d. Thus,

$$\dot{X} = \mathbf{A}X + \mathbf{B}U + \mathbf{G}\Delta W_w \tag{11a}$$

$$R = \mathbf{C}X + V \tag{11b}$$

where

$X = [X_1\ X_2 \cdots X_{17}\ X_{18}]^T$, 18 × 1 state vector

$U = [\Delta U_{BP}\quad \Delta U_F]^T$, 2 × 1 control vector

$R = [\Delta R_{XS}\quad \Delta R_N]^T$, 2 × 1 output vector

$V = [\Delta V_{XS}\quad \Delta V_N]^T$, 2 × 1 measurement noise vector

ΔW_w = stochastic airflow disturbance of the inlet

$\Delta R_{XS} = \Delta X_S + \Delta V_{XS}$

$\Delta R_N = \Delta N + \Delta V_N$

$$\mathbf{A} = \begin{bmatrix} \mathbf{A}_1 & \mathbf{0} & \mathbf{0} \\ \mathbf{B}_{12}\mathbf{C}_1 & \mathbf{A}_2 & \mathbf{0} \\ \mathbf{B}_3\mathbf{C}_1 & -\mathbf{B}_3\mathbf{C}_{12} & \mathbf{A}_3 \end{bmatrix}$$

$$\mathbf{B} = \begin{bmatrix} \mathbf{B}_{21} & \mathbf{0} \\ \mathbf{0} & \mathbf{B}_{22} \\ \mathbf{0} & \mathbf{0} \end{bmatrix}$$

$$\mathbf{C} = \begin{bmatrix} \mathbf{0} & \mathbf{0} & \mathbf{C}_3 \\ \mathbf{0} & \mathbf{C}_{22} & \mathbf{0} \end{bmatrix}$$

$$\mathbf{G} = [\mathbf{B}_{11}\quad \mathbf{0}\quad \mathbf{0}]^T$$

The detail expression of the Jacobian matrices of **A**, **B**, **C**, and **G** are shown in Table 1. The derivation of Eq. (11) is shown in Appendix A.

Solution of the State Space Model of the Combination

Since Eq. (11) is a set of stiff differential equations with a degree of stiffness around 10^2, the dynamic behavior of the combination is solved by combining the Runge-Kutta method and the recursive method of eigenvalue-eigenvector (Appendix B) with different time steps to reach a reasonable computing time. The low-frequency engine model is solved by the former method with a time step of 0.01 s, while the medium-frequency inlet model is solved by the latter method with a time step of 0.001 s (less than 1/10 of the inlet time constant) in order to assure the stability of computation.[15]

Optimal Control

Linear Quadratic Stochastic Optimal Control Problem

The linear time-invariant system described in the state-space expression of Eq. (11) with zero-mean, Gaussian noise vectors $\mathbf{G}\Delta W_w$ and V and their covariances are given by

$$E\{\mathbf{G}\Delta W_w(t)[\mathbf{G}\Delta W_w(t+\tau)^T]\} = \mathbf{Q}_e\delta(\tau) \tag{12a}$$

$$E[V(t)V^T(t+\tau)] = \mathbf{Z}_e\delta(\tau) \tag{12b}$$

$$E[\mathbf{G}\Delta W_w(t)V^T(t+\tau)] = 0 \tag{12c}$$

$$E[\mathbf{G}\Delta W_w(t)] = E[V(t)] = 0 \tag{12d}$$

where

$$\mathbf{Q}_e = \left[\begin{array}{c|c} \mathrm{PSD}(\Delta W_w) & \mathbf{0} \\ \hline \mathbf{0} & \mathbf{0} \end{array}\right]_{18\times 18} \tag{13a}$$

$$\mathbf{Z}_e = \begin{bmatrix} \mathrm{PSD}(\Delta V_{XS}) & 0 \\ 0 & \mathrm{PSD}(\Delta V_N) \end{bmatrix}_{2\times 2} \tag{13b}$$

and $\mathrm{PSD}(\Delta W_w)$, $\mathrm{PSD}(\Delta V_{XS})$, and $\mathrm{PSD}(\Delta V_N)$ are the power spectral densities of ΔW_w, ΔV_{XS}, and ΔV_N, respectively.

Thus, the problem of linear quadratic stochastic optimal control is to select an optimal control vector $U(t)$ to minimize the following quadratic performance index:

$$J = E\left\{\int_0^\infty \tfrac{1}{2}[X^T(\tau)\mathbf{Q}X(\tau) + U^T(\tau)\mathbf{Z}U(\tau)]\,\mathrm{d}\tau\right\} \tag{14}$$

where **Q** is a positive semidefinite weighting matrix and **Z** a positive definite weighting matrix.

Formulation of Performance Index

For inlet control, the normal shock must be maintained downstream of the geometrical throat. Hence, the variance of the shock position increment $E[(\Delta X_S)^2]$ is selected as one term of the performance index. For engine speed control, the increment of speed under any disturbances should be as small as possible. Therefore, the variance of the increment of engine speed $E[(\Delta N)^2]$ is also selected as another term of the performance index. Furthermore, it is hoped to fulfil the control task with a minimum control effort, so that the variance of the increment of the bypass door control voltage $E[(\Delta U_{BP})^2]$ and the variance of the increment of fuel flow $E[(\Delta U_F)^2]$ are selected as the third and fourth terms of the performance index.

Hence, the performance index can be written as

$$J = E\left\{\tfrac{1}{2}\int_0^\infty [K_1\Delta X_S^2 + K_2\Delta N^2 + K_3\Delta U_{BP}^2 + K_4\Delta U_F^2]\,\mathrm{d}t\right\}$$
$$= E\left\{\tfrac{1}{2}\int_0^\infty [X^T\mathbf{Q}X + \mathbf{U}^T\mathbf{Z}U]\,\mathrm{d}t\right\} \tag{15}$$

Table 1 Elements of matrices A, B, C, G

	$-c_{22}$	$-c_{12}$																
	1																	
			$-c_{21}$	$-c_{12}$														
			1															
	d_{22}	d_{12}		d_{11}	$-\mu_{65}$	$-\mu_{55}$	$-\mu_{45}$	$-\mu_{35}$	$-\mu_{25}$	$-\mu_{15}$								
$\mathbf{A} =$																		
						1												
							1											
								1										
									1									
											$-\mu_{26}$	$-\mu_{16}$						
											1							
	d_{22}	d_{12}		d_{11}		$-\mu_{51}$	$-\mu_{41}$	$-\mu_{31}$	$-\mu_{21}$	$-\mu_{11}$	$-\mu_{22}$	$-\mu_{12}$	$-a_{62}$	$-a_{52}$	$-a_{42}$	$-a_{32}$	$-a_{22}$	$-a_{12}$
													1					
														1				
															1			
																1		
																	1	
$\mathbf{B}^T =$	1																	
									1									
$\mathbf{G}^T =$	1																	
$\mathbf{C} =$																		b_{12}
						μ_{53}	μ_{43}	μ_{33}	μ_{23}	μ_{13}	μ_{24}	μ_{14}						

where

$$\mathbf{Q} = \mathbf{C}^T \begin{bmatrix} K_1 & 0 \\ 0 & K_2 \end{bmatrix} \mathbf{C} \quad \text{and} \quad \mathbf{Z} = \begin{bmatrix} K_3 & 0 \\ 0 & K_4 \end{bmatrix}$$

Factors K_1 and K_2 are used to regulate the magnitudes of the two controlled variables and K_3 and K_4 to limit the magnitudes of the two control variables. Every set of K_3 and K_4 can be used to minimize J, but a set composed of different magnitudes of ΔU_{BP} and ΔU_F are required in order that the controller can be designed without control saturation by a suitable choice of K_3 and K_4 if the maximum range in the variation of the two control variables are given.

Optimal Controller Design

In solving the control and estimation problem[16] for a quadratic performance index by the law of separation, the optimal estimate of the state vector and optimal control law can at first be treated separately and then combined into one optimal controller.

The optimal state estimate of the state vector can be generated by a Kalman filter of a continuous system described by

$$\dot{\hat{X}} = \mathbf{A}\hat{X} + \mathbf{B}U + \mathbf{K}_e(R - \mathbf{C}\hat{X}) \tag{16}$$

where

$$\mathbf{K}_e - \mathbf{S}_e\mathbf{C}\mathbf{Z}_e^{-1} \tag{17}$$

is the optimal gain matrix and the variance matrix of estimation errors is the symmetric positive definite solution of the following algebraic Riccati matrix equation:

$$\mathbf{A}\mathbf{S}_e + \mathbf{S}_e + \mathbf{S}_e\mathbf{A}^T - \mathbf{S}_e\mathbf{C}^T\mathbf{Z}_e^{-1}\mathbf{C}\mathbf{S}_e + \mathbf{Q}_e = 0 \tag{18}$$

For a linear quadratic output regulator problem, the optimal feedback control law is designed as

$$U = -\mathbf{Z}^{-1}\mathbf{B}^T\mathbf{S}_c X \tag{19}$$

where $\mathbf{S}_c$ is the symmetric position definite solution of the algebraic Riccati matrix equation

$$\mathbf{S}_c\mathbf{A} + \mathbf{A}^T\mathbf{S}_c - \mathbf{S}_c\mathbf{B}\mathbf{Z}^{-1}\mathbf{B}^T\mathbf{S}_c + \mathbf{Q} = 0 \tag{20}$$

Substituting the optimal state estimate $\hat{X}$ from Eq. (13) for the state vector X of Eq. (19), we have

$$U = -\mathbf{Z}^{-1}\mathbf{B}^T\mathbf{S}\hat{X} = -\mathbf{K}_c\hat{X} \tag{21}$$

where

$$\mathbf{K}_c = \mathbf{Z}^{-1}\mathbf{B}^T\mathbf{S}_c \tag{22}$$

Substituting Eq. (21) into Eq. (16) and rearranging, we have the optimal controller equation

$$\dot{\hat{X}} = (\mathbf{A} - \mathbf{B}\mathbf{K}_c - \mathbf{K}_e\mathbf{C})\hat{X} + \mathbf{K}_e R \tag{23a}$$

$$U = -\mathbf{K}_c\hat{X} \tag{23b}$$

The block diagram of the optimal inlet/engine combination control system is shown in Fig. 5.

Solution of Equations

Equation (23) can be solved by the eigenvalue-eigenvector method for a time-invariant state equation with the following recursive formulas:

$$Y(t_{i+1}) = \mathbf{C}'\mathbf{\Phi}(t_{i+1}) \qquad (i = 0, 1, \ldots, n) \tag{24a}$$

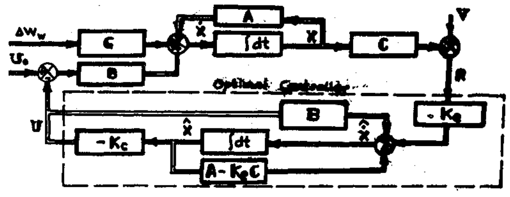

Fig. 5 Block diagram of the optimal control system.

$$\Phi(t_{i+1}) = \mathbf{P}_{cm}(\mathrm{d}t_i)\Phi(t_i) + \mathbf{H}_{cm}(\mathrm{d}t_i)U(t_i) \tag{24b}$$

$$\Phi(0) = \mathbf{X}_0' \tag{24c}$$

where

$$t_{i+1} = t_i + \mathrm{d}t_i$$

$$U(\tau) = U(t_i) = \text{const} \qquad (t_i \le \tau \le t_{i+1}) \tag{25a}$$

$$\mathbf{P}_{cm}(\mathrm{d}t_i) = e^{\mathbf{A}'\mathrm{d}t_i} \tag{25b}$$

$$\mathbf{H}_{cm}(\mathrm{d}t_i) = \int_0^{\mathrm{d}t_i} e^{\mathbf{A}'(\mathrm{d}t_i - v)}\mathbf{B}'\,\mathrm{d}v \tag{25c}$$

The derivation of the above formulas is shown in Appendix B. The algebraic Riccati matrices [Eqs. (18) and (20)] are solved for by Geyser and Lehtinen's digital program.[17]

Digital Simulation Results

The optimal control system, composed of the inlet/engine combination of Eq. (11) and the optimal controller of Eq. (23), is then simulated digitally.

As an example, the NASA 48 cm axisymmetric mixed-compression inlet and the J85-13 turbojet engine are selected. Their steady-state performances are taken from Refs. 13 and 18.

Matrix coefficient values of Eq. (11) for the calculating point of $M_H = 2.462$, $N = 16{,}170$ rpm, $P_H = 1.054$ kg/cm^2, and $T_H = 389.1$ K are shown in Table 2.

Selection of Weighting Factors

The weighting factors K_1, K_2, K_3, and K_4 of the performance index are selected by method of trial and error. First, let K_1 and K_2 be two given values (for example, $K_1 = 1$ and $K_2 = 1$ and thus, $E[(\Delta X_s)^2]$ and $E[(\Delta N)^2]$ have the same weight); then, K_3 and K_4 are selected to assure that the absolute values of the optimal control variables U_{BP} and U_F are less than their maximum allowable values and the variables to be controlled (X_s and N) possess better transient behavior. Since **Q** and **Z** are diagonal matrices, the larger the factors K_3 and K_4, the smaller the relevant control variables, and vice versa. The ranges of K_3 and K_4 are at first roughly determined according to this relation; then, K_3 and K_4 are determined accurately to obtain an even better transient behavior of X_s and N.

After successive tries, a set of weigthing factors is obtained, as

$$K_1 = 1, \quad K_2 = 1, \quad K_3 = 13.48, \quad K_4 = 40.44015$$

Results of Simulation

Figure 6 shows the transient responses of the various parameters due to a 1.4% step increase of the downstream airflow disturbance ΔW_w. In this figure, all of the parameters are shown as percent changes in their initial steady-state values and increase in the upward direction and the "xxx" curves represent the results of this paper. The engine airflow is decreased abruptly to point 1 and the shock is moved downstream rapidly to point 2 (Figs. 6b and 6c). The engine speed increases slowly due to the decrease in the engine airflow (and, therefore, to the decrease in the compressor loading) and its relatively large inertia (Fig. 6d). The slow bypass doors are then closed gradually to offset the change in the engine airflow, as shown in Fig. 6e. The fuel flow decreases slowly due to the action of the fuel control in order to offset the increase in engine speed (Fig. 6f). The compressor discharge pressure also decreases slowly due to the combined effect of the decrease in the engine airflow and the slow increase in the engine speed (Fig. 6g). The turbine inlet gas temperature increases abruptly to point 3 due to the abrupt decrease in the engine airflow and the slow decrease in the fuel flow (Fig. 6h).

After the transient time of 0.01 s, the shock returns slowly from point 2 to its initial position as the result of closing of the bypass doors (Fig. 6c). The engine airflow also increases slowly from the minimum point 1 to the initial value due to the closing of the bypass doors and the increase in the engine speed (Fig. 6b). The fuel flow increases from the minimum point 4 at 0.45 s to the initial value owing to the increase in the engine airflow (Fig. 6f). The compressor discharge pressure appears to have the same transient response as fuel flow, but with a smaller undershoot (Fig. 6g). The turbine inlet gas temperature shows no evident change from 0.02 to 0.8 s and then decreases slowly to the initial value owing to the combined effect of change of the engine airflow and fuel flow (Fig. 6h). Hence, the transient responses of the two controlled variables (X_s and N) fulfill the requirements of the performance criterion. Also, the results

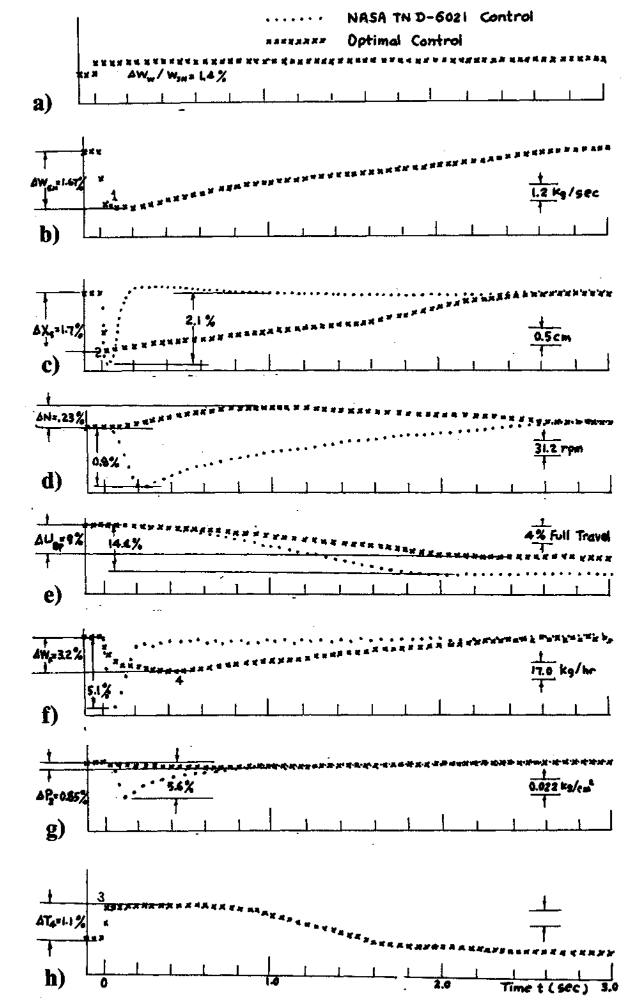

Fig. 6 Transient responses of parameters of the integrated control system: a) downstream airflow disturbance ΔW_w; b) engine airflow ΔW_{EN}; c) shock position ΔX_s; d) engine speed ΔN; e) bypass door control ΔU_{BP}; f) fuel flow rate ΔW_F; g) compressor discharge pressure ΔP_3; h) turbine inlet gas temperature ΔT_4.

Table 2 Element values of matrices A, B, G, C

A =	5.000×10^3	-1.4286																
	0.35×10^3																	
			-628	-1.1268×10^3														
			350															
	0.1	1.4286		2.3417×10^2	-4.1682×10^5	-5.289×10^5	-6.3224×10^3	-1.5968×10^5	-1.3403×10^3	-2.0387								
						350												
							350											
								350										
									350									
											-3.0223	-4.6258×10^{-3}						
											350							
	0.1	1.4286		2.3417×10^3		-344.32	-691.37	-579.37	-504.31	-1.6783	-78.585	-0.2626	-1.0563×10^3	-3.6515×10^3	-8.4613×10^3	-8.5232×10^2	-8.6201×10^3	-1.858×10^3
													350					
														350				
															350			
																350		
																	350	
$B^T =$			350								350							
$G^T =$	350																	
C =						110.65	222.18	186.18	162.06	0.5393	25.254	0.0844						18.871

show that the shock position X_S and the speed N can be maintained at their optimal values simultaneously by the optimal control of the combination.

Benefits of the Optimal Control

The dotted lines of Fig. 6 were the responses of a cross-coupled control for the same NASA 48 cm inlet/J85 engine combination. The system employed manipulation of the fuel flow to control engine speed and both bypass door area (as a reset) and engine speed (as a primary variable) to control the shock position. A comparison of the responses of the optimal control (solid lines) and the conventional control (dash-dot lines) shows that the overshoot of engine speed for the optimal control is four times less than that of the conventional control, while the returning action of the shock position is much smoother for the optimal control than that of the conventional control; thus, the stability of the optimal control system is much better than that of the conventional control.

Conclusions

It was demonstrated that a linear quadratic stochastic, two-variable control system of the integrated inlet/engine combination can be designed by modern optimal control theory.

The results of the sample simulation show that the transient behavior of the two controlled variables (the normal shock position and engine speed) can be maintained at their optimal predetermined values simultaneously by suitable selection of the weighting factors of the performance index, while the dynamic performance of the optimal control is much better than the conventional cross-coupled control.

This theoretical design method can also be extended to the case of a multivariable system. Of course, the degree of complexity of the mathematical model of such a control system and the computational requirement of the control will be increased sharply.

Appendix A: Derivation of State Space Model of the Inlet/Engine Combination

State-Space Expression of Block I of Fig. 3c

Equation (5) can be transferred into the standard state-space expression as

$$\begin{bmatrix}\dot{X}_1\\ \dot{X}_2\end{bmatrix} = \begin{bmatrix}-C_{22} & -C_{12}\\ 1 & 0\end{bmatrix}\begin{bmatrix}X_1\\ X_2\end{bmatrix} + \begin{bmatrix}1\\ 0\end{bmatrix}\Delta W_w \tag{A1a}$$

$$\Delta W_{NS} = [d_{22} \quad d_{12}]\begin{bmatrix}X_1\\ X_2\end{bmatrix} \tag{A1b}$$

In the same manner, Eq. (6) can be transferred into

$$\begin{bmatrix}\dot{X}_3\\ \dot{X}_4\end{bmatrix} = \begin{bmatrix}-C_{21} & -C_{11}\\ 1 & 0\end{bmatrix}\begin{bmatrix}X_3\\ X_4\end{bmatrix} + \begin{bmatrix}1\\ 0\end{bmatrix}\Delta U_{\mathrm{BP}} \tag{A2a}$$

$$\Delta W_c = [0 \quad d_{11}]\begin{bmatrix}X_3\\ X_4\end{bmatrix} \tag{A2b}$$

From Fig. 4a,

$$\Delta W_{\mathrm{BP}} = \Delta W_c + \Delta W_{NS} \tag{A3}$$

Combining Eqs. (A1–A3), we have the state-space expression of block 1,

$$\dot{\boldsymbol{X}}_1 = \mathbf{A}_1 \boldsymbol{X}_1 + \mathbf{B}_1 \boldsymbol{U}_1 \tag{A4a}$$

$$\mathbf{Y}_1 = \mathbf{C}_1 \boldsymbol{X}_1 \tag{A4b}$$

where

$$\boldsymbol{X}_1 = [X_1 \quad X_2 \quad X_3 \quad X_4]^T \tag{A5a}$$

X_1, X_2, X_3, X_4 = state variables of bypass door and actuator noise

$$Y_1 = \Delta W_{BP} \tag{A5b}$$

$$U_1 = [\Delta W_w \quad \Delta U_{BP}]^T \tag{A5c}$$

$$\mathbf{A}_1 = \begin{bmatrix} -C_{22} & -C_{12} & 0 & 0 \\ 1 & 0 & 0 & 0 \\ 0 & 0 & -C_{21} & -C_{11} \\ 0 & 0 & 1 & 0 \end{bmatrix} \tag{A5d}$$

$$\mathbf{B}_1 = [\mathbf{B}_{11} \quad \mathbf{B}_{21}] \tag{A5e}$$

$$\mathbf{B}_{11} = [1 \quad 0 \quad 0 \quad 0]^T$$

$$\mathbf{B}_{21} = [0 \quad 0 \quad 1 \quad 0]^T$$

$$\mathbf{C}_1 = [d_{22} \quad d_{12} \quad 0 \quad d_{11}] \tag{A5f}$$

State-Space Expression of Block II of Fig. 3c

Applying the principle of linear superposition to Fig. 2b, we have the expression

$$\begin{bmatrix} \Delta W_{EN} \\ \Delta N \end{bmatrix} = \begin{bmatrix} h_{11} & h_{12} \\ h_{21} & h_{22} \end{bmatrix} \begin{bmatrix} \Delta W_{BP} \\ \Delta U_F \end{bmatrix} \tag{A6}$$

where

$$h_{11} = K_N G_{IN,1} G_{EN,1}$$
$$h_{12} = K_F K_N G_{EN,2}$$
$$h_{21} = G_{IN,1} G_{EN,1}$$
$$h_{22} = G_{EN,2}$$

Equation (A6) can be transferred into

$$\dot{X}_2 = \mathbf{A}_2 X_2 + \mathbf{B}_2 U_2 \tag{A7a}$$

$$Y_2 = \mathbf{C}_2 X_2 \tag{A7b}$$

where

$$X_2 = [X_5 \quad X_6 \quad X_7 \cdots X_{11} \quad X_{12}]^T$$

$$U_2 = [\Delta W_{BP} \quad \Delta W_F]^T, \quad \mathbf{Y}_2 = [\Delta W_{EN} \quad \Delta N]^T$$

$$\mathbf{A}_2 = \begin{bmatrix} \mathbf{A}_{12} & \mathbf{0} \\ \mathbf{0} & \mathbf{A}_{22} \end{bmatrix}, \quad \mathbf{B}_2 = [\mathbf{B}_{12} \quad \mathbf{B}_{22}], \quad \mathbf{C}_2 = \begin{bmatrix} \mathbf{C}_{12} \\ \mathbf{C}_{22} \end{bmatrix}$$

$$\mathbf{A}_{12} = \begin{bmatrix} -\mu_{65} & -\mu_{55} & -\mu_{45} & -\mu_{35} & -\mu_{25} & -\mu_{15} \\ 1 & & & & & \\ & 1 & & & \mathbf{0} & \\ & & 1 & & & \\ & \mathbf{0} & & 1 & & \\ & & & & 1 & 0 \end{bmatrix}$$

$$\mathbf{A}_{22} = \begin{bmatrix} -\mu_{26} & -\mu_{16} \\ 1 & 0 \end{bmatrix}$$

$$\mathbf{B}_{12} = [1 \quad 0 \quad 0 \quad \cdots \quad 0]^T_{8 \times 1}$$

$$\mathbf{B}_{22} = [0 \quad 0 \quad 0 \quad \cdots \quad 1]^T_{8 \times 1}$$

$$\mathbf{C}_{12} = [0 \quad \mu_{51} \quad \mu_{41} \quad \mu_{31} \quad \mu_{21} \quad \mu_{11} \quad \mu_{22} \quad \mu_{12}]_{8 \times 1}$$

$$\mathbf{C}_{22} = [0 \quad \mu_{53} \quad \mu_{43} \quad \mu_{33} \quad \mu_{23} \quad \mu_{13} \quad \mu_{24} \quad \mu_{14}]_{8 \times 1} \tag{A8}$$

where μ_{65}, $\mu_{55} \cdots$ are elements of the matrices $\mathbf{A}_{12}$, $\mathbf{A}_{22}$, $\mathbf{B}_{12}$, $\mathbf{B}_{22}$, $\mathbf{C}_{12}$, $\mathbf{C}_{22}$ [functions of coefficients $a_{11}, a_{12}, \ldots, a_{61}, a_{51}, \ldots$ of Eqs. (1) and (3)].

State Space Expression of Block III of Fig. 3c

Equation (2) can be transferred into

$$\dot{X}_3 = \mathbf{A}_3 X_3 + \mathbf{B}_3 U_3 \tag{A9a}$$

$$Y_3 = \mathbf{C}_3 X_3 \tag{A9b}$$

where

$$X_3 = [X_{13} \quad X_{14} \quad X_{15} \quad X_{16} \quad X_{17} \quad X_{18}]^T$$

$$Y_3 = \Delta X_S$$

$$U_3 = \Delta W_{JN}$$

$$\mathbf{A}_3 = \begin{bmatrix} -a_{62} & -a_{52} & -a_{42} & -a_{32} & -a_{22} & -a_{12} \\ 1 & & & & & \\ & 1 & & & \mathbf{0} & \\ & & 1 & & & \\ & \mathbf{0} & & 1 & & \\ & & & & 1 & \\ & & & & & 1 \end{bmatrix}$$

$$\mathbf{B}_3 = [1 \quad 0 \quad 0 \quad 0 \quad 0 \quad 0]^T$$

$$\mathbf{C}_3 = [0 \quad 0 \quad 0 \quad 0 \quad 0 \quad b_{12}] \tag{A10}$$

State-Space Expression of the Inlet/Engine Combination

Combining Eqs. (A4), (A7), and (A9) and also considering Eq. (A10), the required Eq. (11) of the state-space expression of the combination can be obtained.

Appendix B: Derivation of Recursive Method of Eigenvalue-Eigenvector

For a linear time-invariant system,

$$\dot{X} = \mathbf{A}X + \mathbf{B}U \tag{A11a}$$

$$Y = \mathbf{C}X \tag{A11b}$$

If the case of general eigenvectors of **A** [i.e., suppose **A** consists of n (order of **A**) independent eigenvectors] is not considered, then the following solution can be used.

Solution of State Transition Matrix

When the initial state vector is X_0, the solution of Eq. (A11) will be

$$Y(t) = \mathbf{C}\left\{e^{\mathbf{A}t}X_0 + \int_0^t e^{\mathbf{A}(t-\tau)}\mathbf{B}U(\tau)\,\mathrm{d}t\right\} \tag{A12}$$

Let $\lambda_1, \ldots, \lambda_i, \lambda_{i+1}, \ldots, \lambda_n$ and $\mathbf{r}_1, \mathbf{r}_2, \ldots, \mathbf{r}_i, \mathbf{r}_{i+1}, \ldots, \mathbf{r}_n$ are eigenvalues and eigenvectors of matrix **A**, respectively. While λ_i and λ_{i+1} are a pair of corresponding conjugate eigenvectors.

In order to avoid computation of complex numbers and, thus, to save computer time, the real and imaginary parts of the complex conjugate eigenvectors of **A** can be written separately as

$$\boldsymbol{r}_i = \boldsymbol{r}_{rei} + j\boldsymbol{r}_{Imi} \quad \text{(A13a)}$$

$$\boldsymbol{r}_{i+1} = \boldsymbol{r}_{Rei} - j\boldsymbol{r}_{Imi} \quad \text{(A13b)}$$

and let

$$\boldsymbol{r}'_i = \boldsymbol{r}_{Rei} + \boldsymbol{r}_{Imi} \quad \text{(A14a)}$$

$$\boldsymbol{r}'_{i+1} = \boldsymbol{r}_{Rei} - \boldsymbol{r}_{Imi} \quad \text{(A14b)}$$

then

$$\mathbf{A} = [\boldsymbol{r}'_i \quad \boldsymbol{r}'_{i+1}] = [\boldsymbol{r}_i \quad \boldsymbol{r}_{i+1}] \begin{bmatrix} \theta_i & -\eta_i \\ \eta_i & \theta_i \end{bmatrix}$$

where θ_i and η_i are determined from

$$\lambda_i = \theta_i + j\eta_i \quad \text{(A15a)}$$

$$\lambda_{i+1} = \theta_i - j\eta_i \quad \text{(A15b)}$$

Substitute for the ith and $(i+1)$st column, $\boldsymbol{r}_i$ and $\boldsymbol{r}_{i+1}$, of the eigenvector matrix $\mathbf{T}_v$ with $\boldsymbol{r}'_i$ and $\boldsymbol{r}'_{i+1}$, respectively, and all other complex conjugate eigenvectors of $\mathbf{T}_v$ are substituted in the same way. Thus, a new real eigenvector matrix $\mathbf{T}'_v$ is formulated. Take $\mathbf{T}'_v$ as a linear transformation matrix of

$$X = \mathbf{T}'_v X'$$

and Eqs. (A11) can be transformed into

$$\dot{X}' = \mathbf{A}'X' + \mathbf{B}'U \quad \text{(A16a)}$$

$$Y = \mathbf{C}'X' \quad \text{(A16b)}$$

where

$$\mathbf{A}' = (\mathbf{T}'_v)^{-1}\mathbf{A}\mathbf{T}'_v$$

$$\mathbf{B}' = (\mathbf{T}'_v)^{-1}\mathbf{B}$$

$$\mathbf{C}' = \mathbf{C}\mathbf{T}'_v$$

$$\mathbf{A}' = \begin{bmatrix} \lambda_1 & & & & & & \\ & \ddots & & & & & \\ & & \lambda_{i-1} & & & & \\ & & & \theta_i & -\eta_i & & \\ & & & \eta_i & \theta_i & & \\ & & & & & \lambda_{i+1} & \\ & & & & & & \ddots \\ & & & & & & & \lambda_n \end{bmatrix} \quad \text{(A17)}$$

From Eqs. (A12) and (A17), solution Y can be rewritten as

$$Y = \mathbf{C}'\left[e^{\mathbf{A}'t}X'_0 + \int_0^t e^{\mathbf{A}'(t-\tau)}\mathbf{B}'U(\tau)\,\mathrm{d}\tau\right] \quad \text{(A18)}$$

where

$$X'_0 = (\mathbf{T}'_v)^{-1}X_0 \quad \text{(A19)}$$

$$e^{\mathbf{A}'t} = \begin{bmatrix} e^{\lambda_1 t} & & & & & \\ & \ddots & & & & \\ & & e^{\lambda_{i-1} t} & & & \\ & & & e^{\begin{bmatrix} \theta_i & -\eta_i \\ \eta_i & \theta_i \end{bmatrix} t} & & \\ & & & & e^{\lambda_{i+2} t} & \\ & & & & & \ddots \\ & & & & & & e^{\lambda_n t} \end{bmatrix} \quad \text{(A20)}$$

and

$$e^{\begin{bmatrix} \theta_i & -\eta_i \\ \eta_i & \theta_i \end{bmatrix} t} = \begin{bmatrix} e^{\theta_i t}\cos(\eta_i t) & -e^{\theta_i t}\sin(\eta_i t) \\ e^{\theta_i t}\sin(\eta_i t) & e^{\theta_i t}\cos(\eta_i t) \end{bmatrix} \quad \text{(A21)}$$

Recursive Computation Formulas

In order to save computer time further, a recursive computation formula of $Y(t)$ is deduced to obtain direct numerical integration of $Y(t)$ from Eq. (A18).

Suppose $Y(t_i)$ at time t_i is known. Let

$$Y(t_i) = \mathbf{C}'\boldsymbol{\Phi}(t_i) \quad \text{(A22a)}$$

where

$$\boldsymbol{\Phi}(t_i) = e^{\mathbf{A}'t_i}X'_0 + \int_0^{t_i} e^{\mathbf{A}'(t_i-\tau)}\mathbf{B}'U(\tau)\,\mathrm{d}\tau \quad \text{(A22b)}$$

Let

$$t_{i+1} = t_i + \mathrm{d}t_i$$

where $\mathrm{d}t_i$ is the time step. Then, from Eq. (A22)

$$Y(t_{i+1}) = \mathbf{C}'\boldsymbol{\Phi}(t_{i+1}) \quad \text{(A23a)}$$

where

$$\boldsymbol{\Phi}(t_{i+1}) = e^{\mathbf{A}'\mathrm{d}t_i}\boldsymbol{\Phi}(t_i) + \int_{t_i}^{t_i+\mathrm{d}t_i} e^{\mathbf{A}'(t_i+\mathrm{d}t_i-\tau)}\mathbf{B}'U(\tau)\,\mathrm{d}\tau \quad \text{(A23b)}$$

By the transformation of

$$v = \tau - t_i \quad \text{(A24)}$$

We have

$$\mathrm{d}v = \mathrm{d}\tau \quad \text{(A25)}$$

where t_i is the initial value.

Substituting Eqs. (A24) and (A25) into Eq. (A23), we have

$$\boldsymbol{\Phi}(t_{i+1}) = e^{\mathbf{A}'\mathrm{d}t_i}\boldsymbol{\Phi}(t_i) + \int_0^{\mathrm{d}t_i} e^{\mathbf{A}'(\mathrm{d}t_i-v)}\mathbf{B}'U(t_i+v)\,\mathrm{d}v \quad \text{(A26)}$$

From Eq. (A22), initial value of $\boldsymbol{\Phi}(0)$ is determined by

$$\boldsymbol{\Phi}(0) = e^{\mathbf{A}'0}X'_0 + \int_0^0 e^{\mathbf{A}'(0-\tau)}\mathbf{B}'U(\tau)\,\mathrm{d}\tau = X'_0 \quad \text{(A27)}$$

In general, the control vector $U(\tau)$ satisfies the condition

$$U(\tau) = U(t_i) = \text{const vector } (t_i \le \tau \le t_{i+1}) \quad \text{(A28)}$$

Then, Eq. (A22) becomes

$$\boldsymbol{\Phi}(t_{i+1}) = e^{\mathbf{A}'\mathrm{d}t_i}\boldsymbol{\Phi}(t_i) + \int_0^{\mathrm{d}t_i} e^{\mathbf{A}'(\mathrm{d}t_i-v)}\mathbf{B}'\,\mathrm{d}v\,U(t_i)$$

$$= \mathbf{P}_{cm}(\mathrm{d}t_i)\boldsymbol{\Phi}(t_i) + \mathbf{H}_{cm}(\mathrm{d}t_i)U(t_i) \quad \text{(A29)}$$

where

$$P_{cm}(dt_i) = e^{A'dt_i} \quad \text{(A30a)}$$

$$H_{cm}(dt_i) = \int_0^{dt_i} e^{A'(dt_i - v)} B' \, dv \quad \text{(A30b)}$$

Apparently, P_{cm} and H_{cm} depend upon time step dt_i only.

Combining Eqs. (A22) and (A27) to (A30), we have the recursive computation equations (24) and (25).

References

[1]Cole, G. L. Neiner, G. H., and Wallhangen, R. E, "Coupled Supersonic Inlet-Engine Control Using Overboard Bypass Doors and Engine Speed to Control Normal Shock Position," NASA TN D-6019, 1970.

[2]Paulovich, F. J., Neiner, G. H., and Hagodorn, R. E., "A Supersonic Inlet-Engine Control Using Engine Speed as a Primary Variable for Controlling Normal Shock Position," NASA TN D-6021, 1971.

[3]Baumbick, R. J., Batterton, P. G., and Daniele, C. J., "Terminal Shock and Restart Control of a Mach 2.5, Mixed-Compression Inlet Coupled to a Turbofan Engine," NASA TM X-3104, 1974.

[4]Lehtinen, B., Zeller, J. R., and Geyer, L. C., "Optimal Control of Supersonic Inlets to Minimize Unstart," NASA TN D-6408, 1971.

[5]Zeller, J. R., Lehtinen, B., Geyer, L. C., and Batterton, P. G., "Analytical and Experimental Performance of Optimal Controller Designs for a Supersonic Inlet," NASA TN D-7188, 1973.

[6]Seidel, R. C. and Lehtinen, B., "Control System Design Using Frequency Models and Parameter Optimization, with Application to Supersonic Inlet Controls," NASA TM X-3108, 1974.

[7]Zeller, J. R., "The Role of Modern Control Theory in the Design of Controls of Aircraft Turbine Engine," AIAA Paper 82-0320, 1982.

[8]DeHoff, R. L. and Hall, W. E. Jr., "Optimal Control of Turbine Engine," *Transactions of ASME, Journal of Dynamic Systems, Measurement and Control*, June 1979.

[9]Skira, C. A., DeHoff, R. L., and Hall, W. E., "Design, Evaluation and Test of an Electronic Multivariable Control for the F100 Turbofan Engine," System Control, 1980.

[10]Lee, T. C. and Guan, Y. S., "Optimal Control of Change of State of Aircraft Turbine Engine," ASME Paper 85-IGT-53, 1985.

[11]Guan, Y. S., Yarng, S., and Yarng, J. B., "A Linear Multivariable Dynamical Model of Supersonic Inlet-Engine Combination," AIAA Paper 84-1496, 1984 (also *Journal of Propulsion and Power*, Vol., Nov./Dec. 1985, pp. 477–484.

[12]Willoh, R. G., "A Mathematical Analysis of Supersonic Inlet Dynamics," NASA TN D-4969, 1968.

[13]Stone, C. R., Miller, N. E., and Ward, M. D., "Turbine Engine Control Synthesis, Vols. I and II, AFAPL-TR-75–14, 1975.

[14]Guan, Y. S. and Zhang, S. X., "Mathematical Model of Aircraft Gas Turbine Engine and Its Digital Simulation," Northwestern Polytechnical University, Xi'an, China, 1982.

[15]Yarng, J. B. and Guan, Y. S., "A Dynamic Model of a Supersonic Inlet-Engine Combination and Its Optimal Control," Master Degree Thesis. Northwestern Polytechnical University, Xi'an, China, 1984 (in Chinese).

[16]Bryson, A. E. Jr. and Ho, Y. C., *Applied Optimal Control*, Blaisdell Publishing, 1969.

[17]Geyser, L. C. and Lehtinen, B., "Digital Program for Solving the Linear Stochastic Optimal Control and Estimation Problem," NASA TN D-7820, 1975.

[18]Cubbison, R. W., Meleason, E. T., and Johnson, D. F., "Performance Characteristics from Mach 2.58 to 1.98 of an Axisymmetric, Mixed Compression Inlet System with 60 Percent Internal Contraction," NASA TM X-1739, 1969.